Supplementary Information (SI) for Journal of Materials Chemistry A.
This journal is © The Royal Society of Chemistry 2025

Supplementary Information

"Cyano group bridge"-based enabling high zinc-ion transference number and cycling stability of aqueous zinc-ion batteries

Yuting Jiang, Die Luo, Chen Peng, Ben Niu, Ping Gan, Xianru He*

School of New Energy and Materials, Southwest Petroleum University, Chengdu, Sichuan 610500, China

Corresponding author: Prof. Xianru He
E-mail: xrhe@swpu.edu.cn

Experimental section

Materials. Acrylonitrile (AN) was passed through an Al_2O_3 column before polymerization to eliminate the inhibitor. 2,2'-Azobis[2-(2-imidazolin-2-yl)propane] dihydrochloride (AIBI) was purchased from Shandong Xiya. Acrylamide (AM) was obtained from Shandong Sainuo. Vanadium oxide (V_2O_5, 99%) was purchased from Macklin. Zn (thickness 100 μm), Cu sheets (thickness 100 μm), carbon cloth, polyvinylidene difluoride (PVDF), N-methyl-2-pyrrolidone (NMP) and acetylene black were purchased from Canrd Technology Co. Ltd. Zinc triflate (98%), or ($Zn(OTf)_2$), was obtained from Shanghai Aladdin.

Synthesis of PMN_{-x}. In 50 mL Schlenk flasks, AM (3.79 g, 4.21 g, 4.62 g, 4.79 g, 4.81 g, 4.85 g), AN (1.21 g, 0.79 g, 0.38 g, 0.21 g, 0.19 g, 0.15 g), AIBI (0.125 g), H_2O (27 mL) and C_2H_5OH (18 mL) were mixed under stirring for 30 min. Then the flask was sealed and purged with high-purity nitrogen for 30 min, and the reaction was carried out in oil baths at 50°C for 8 h. After concentrating the solution, these products were precipitated three times in ethanol. These final products were dried in a vacuum oven at 60°C for 24 h before use.

Preparation of electrolyte solution. By dissolving stoichiometric $Zn(OTf)_2$ in deionized water, a 3 M pristine electrolyte aqueous solution was prepared. The PMN_{-x}-containing electrolytes solution were prepared by adding 0.05 wt.%, 0.10 wt.%, 0.15 wt.%, 0.20 wt.% and 0.25% wt.% PMN_{-x} into 3 M $Zn(OTf)_2$ aqueous solution. The weight percentage (wt.%) represents the weight percentage of PMN_{-x} in electrolyte.

Preparation of $Na_2V_6O_{16}\cdot 1.5H_2O$ (NVO) Cathode. According to published literatures[1,2], V_2O_5 cathode material was synthesized. The 3 g of V_2O_5 were dissolved in 45 mL of 2 M sodium chloride (NaCl) aqueous solution and stirred for 72 h. The orange-red gel was obtained, and then washed three times with deionized water and ethanol to remove excess V_2O_5. The resulting product was dried in an oven at 60°C for 12 h.

Material characterization. The molecular weight of copolymers was determined by ambient gel chromatography (Agilent PL-GPC50). Fourier transform infrared spectroscopy (FTIR) was recorded on the Thermo Fisher Scientific Nicolet iS20 instrument. X-ray diffraction (XRD) measurements were performed on a Rigaku Ultima IV diffractometer. The morphologies and element mapping were observed on a ZEISS EVO/MA 15 scanning electron microscope (SEM) with an energy dispersive spectroscopy (EDS). The surface roughness morphology was obtained by the Bruker Atomic Force Microscope (AFM). The surface compositions of Zn anodes were investigated on Nexsa X-ray photoelectron spectroscopy (XPS). The ion conductivity of PMN_{-x}-containing electrolyte at different concentrations was collected through a conductivity meter (YOKE, DDS-307A). Proton nuclear magnetic resonance spectra (^1H NMR) were obtained on a Bruker AVANCE III HD 400 MHz spectrometer. The

hydrodynamic diameters (D_h) of copolymers were measured on Brookhaven Instruments BI-200SM laser scatterometer with a digital correlator (BI-9001). The contact angles between Zn-metal and different electrolytes were measured on an Dataphysics OCA25 optical contact angle goniometer. The specific viscosity (η_{sp}) of PMN_{-x} with different concentrations in aqueous solution was measured by Ubbelohde viscometer. The average capillary diameter of the Ubbelohde viscometer used is 0.41 mm. According to Poiseuille equation:

$$\eta_{sp} = t/t_0 - 1 \quad \text{(S1)}$$

where t is the outflow time of PMN_{-5} solution, t_0 is the outflow time of water, the η_{sp} can be calculated.

Electrochemical Tests. Zn-Zn symmetric cell, Zn-Cu asymmetric cell and Zn-NVO full battery were assembled with CR2032 coin, glass fiber as separator, 3 M $Zn(OTf)_2$ as electrolyte, Zn, Cu and NVO coated carbon cloth as positive electrode with or without copolymer additive. The preparation of NVO cathode is as follows. NVO, acetylene black and polyvinylidene fluoride (PVDF) were compounded into slurry at a mass ratio of 7:2:1. The slurry was coated on a carbon cloth (0.35 mm thick) with a scraper, and then it was cut into a round piece with a diameter of 8 mm, and vacuum dried at 60°C for 24 h. The cycling performance of battery was tested by a Neware battery cycler (CT-4008T-5V10mA-164, Shenzhen, China). Tafel curves were obtained from Zn-Zn symmetric cells using pristine and PMN_{-x}-containing electrolytes. Linear sweep voltammetry (LSV) and cyclic voltammetry (CV) and were carried on CHI660E electrochemical workstation. The chronoamperometry (CA) of Zn-Zn symmetric cells were recorded at a scan rate of 10 mV s^{-1} and an overpotential of -150 mV. In-situ electrochemical impedance spectra (EIS) were carried on a Gamry Reference 3000 electrochemical workstation. The Zn-NVO battery was tested in 3 M pristine electrolyte and PMN_{-5}-containing electrolyte with NVO as the positive electrode and Zn-metal as the negative electrode.

Figures

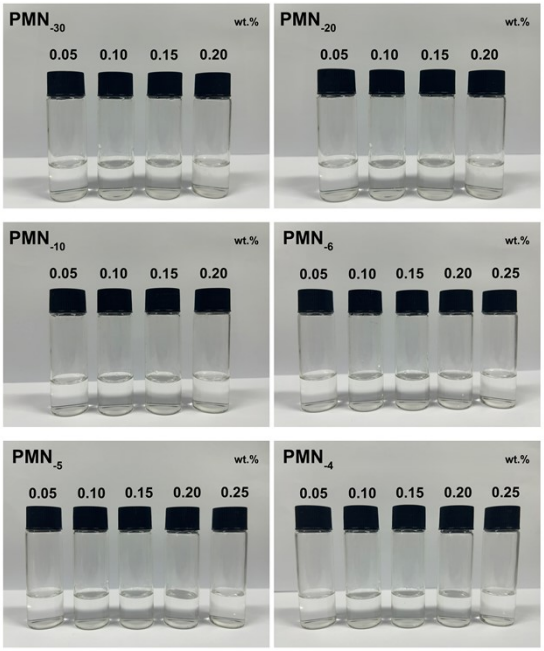

Fig. S1. The dissolution state of PMN_{-x} dissolved in pristine electrolyte with different compositions and concentrations.

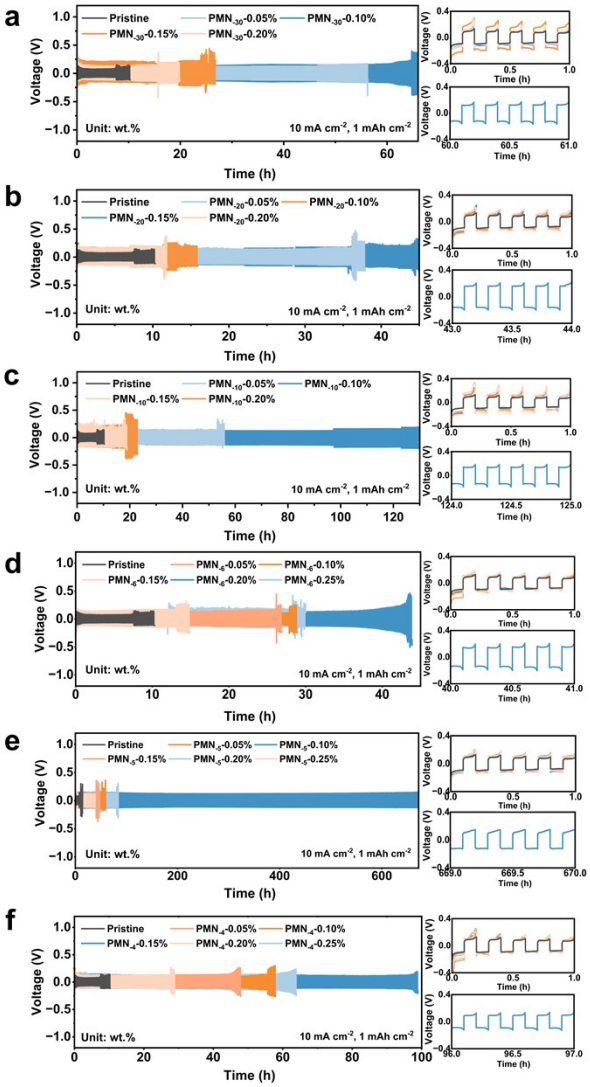

Fig. S2. Cycling performance of Zn-Zn symmetric cells using PMN_{-x}-containing electrolyte at a current density of 10 mA cm^{-2} with a capacity of 1 mAh cm^{-2}.

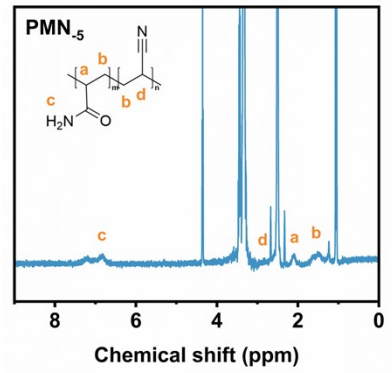

Fig. S3. ^{1}H NMR spectrum of PMN_{-5} with peak assignments.

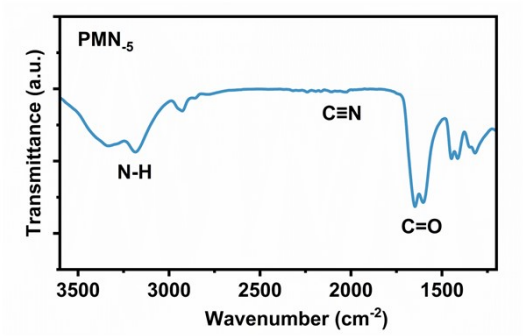

Fig. S4. FTIR spectrum of PMN_{-5} with peak assignments.

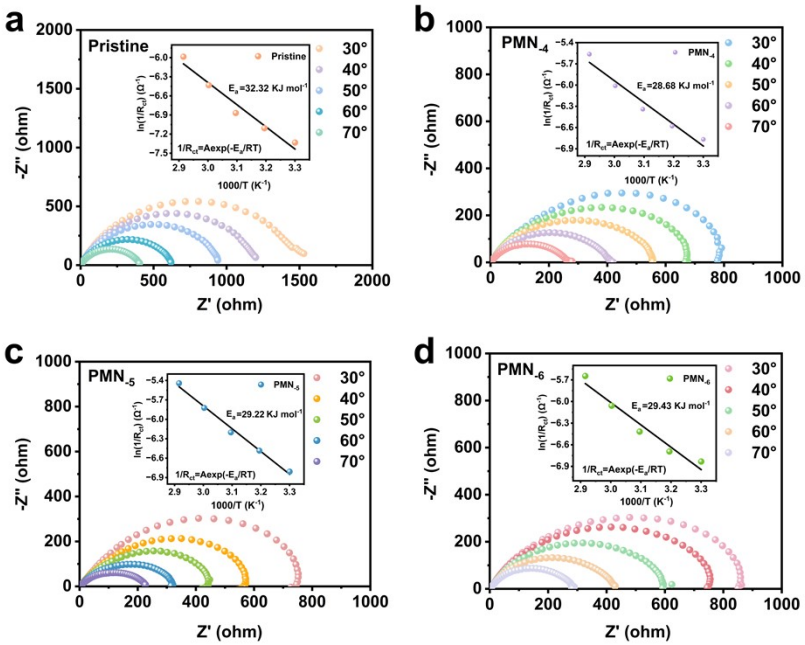

Fig. S5. Electrochemical impedance spectra (EIS) of Zn-Zn symmetric cells with PMN_{-x} electrolyte were obtained between 303 K and 343 K to derive the Arrhenius curve and activation energy E_a.

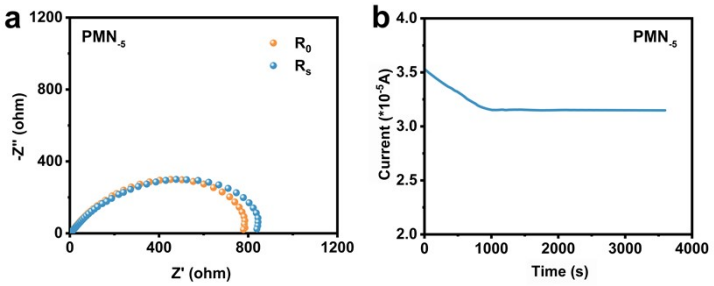

Fig. S6. (a) Electrochemical impedance spectra and (b) chronoamperometry (CA) of Zn-Zn symmetric cells with PMN_{-5}-containing electrolyte.

I_0=3.52*10^{-5} A, I_s=3.13*10^{-5} A, R_0=957.1 Ω, R_s=1026 Ω. By the formula,

$$t_{Zn^{2+}} = I_s(\Delta V - I_0R_0)/I_0(\Delta V - I_sR_s) \quad \text{(S2)}$$

the Zn^{2+} transference number (t_{Zn2+}) can be calculated as 0.87.

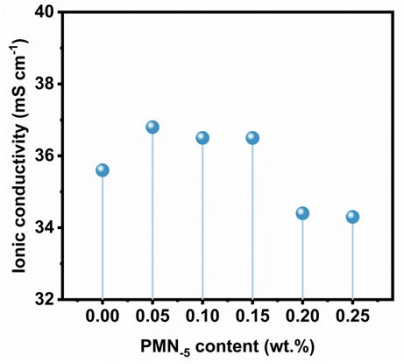

Fig. S7. Ionic conductivity of PMN_{-5}-containing electrolytes at different concentrations.

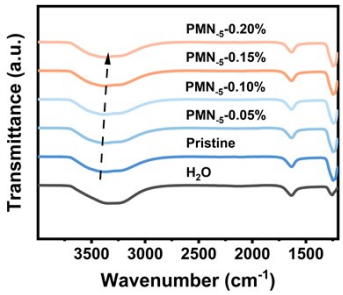

Fig. S8. FTIR spectra of different PMN_{-5} concentration electrolytes in H_2O.

The FTIR spectra shows that after adding pristine electrolyte to pure water, the O-H stretching vibration happened a blue shift and the intensity decreased. This indicates that the hydrogen bond network between water molecules is disrupted and the hydrogen bonding interaction is weakened. While after introducing PMN_{-5}, a red shift in the O-H stretching vibration can be observed. This is due to the enhanced hydrogen bonding interactions between water molecules in electrolyte solution, indicating an increase in the amount of free water.

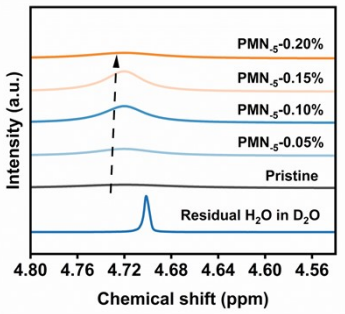

Fig. S9. ^1H NMR spectra of pristine and PMN_{-5}-containing electrolytes with different PMN_{-5} amounts in D_2O.

The ^1H NMR spectra shows that the chemical shift moved from 4.700 ppm to 4.722 ppm in pristine electrolyte solution of 3 M $Zn(OTf)_2$, which indicates that the coordination of Zn^{2+} with D_2O weakens the electron density of D_2O molecules. Compared with pristine electrolyte solution, the chemical shift of PMN_{-5}-containing electrolyte changed from 4.722 ppm to 4.719 ppm, and the chemical shift decreases with the increase of concentration, indicating that the coordination of Zn^{2+} with water is inhibited.

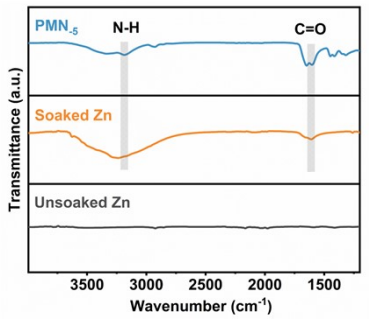

Fig. S10. FTIR spectra of PMN_{-5}, Zn sheets with soaked for 7 days in PMN_{-5}-containing electrolyte, and unsoaked Zn.

The Zn sheet soaked in electrolyte PMN_{-5}-containing has similar spectrum to original PMN_{-5}, indicating that the copolymer additive has adsorption effect on Zn surface. In addition, the blue shift of C=O peak occurs after the original Zn sheet soaking in PMN_{-5}-containing electrolyte, which is due to the interaction between Zn and the polar amide groups in PMN_{-5}, demonstrating the chemical adsorption of PMN_{-5} additive on Zn sheet surface.

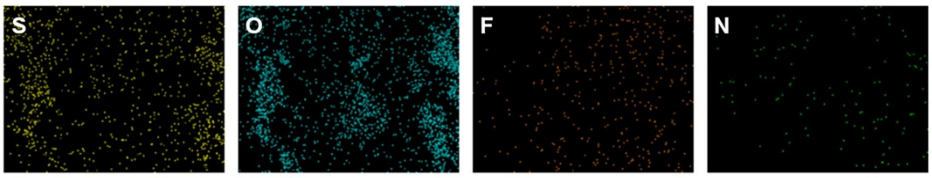

Fig. S11. Energy dispersive spectroscopy (EDS) mapping of Zn sheet soaked in PMN_{-5}-containing electrolyte.

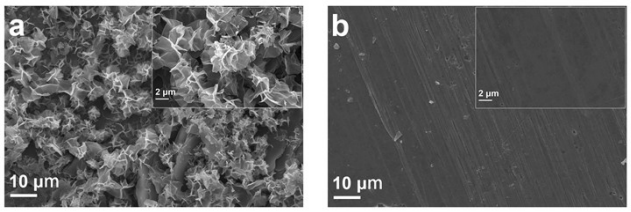

Fig. S12. SEM images of Zn sheet soaking in (a) pristine electrolyte and (b) PMN_{-5}-containing electrolyte for 7 days under 25°C.

Lots of irregular dendrites appeared on the surface of Zn sheet after soaking in pristine electrolyte. While in PMN_{-5}-containing electrolyte, the surface of Zn sheet is smooth and there are scattered small particles.

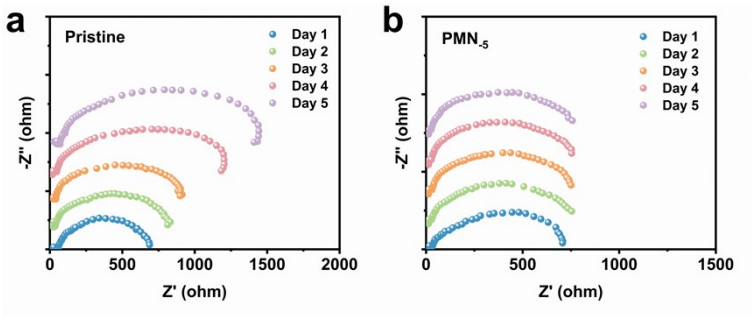

Fig. S13. The EIS curves of Zn-Zn symmetric cells with (a) pristine and (b) PMN_{-5}-containing electrolyte after 1~5 days of laying aside.

The impedance of Zn-Zn symmetric cell with pristine electrolyte increases as the increase of laying aside time. This is due to the accumulation of by-products that formed by the reaction of Zn anode surface with water in pristine electrolyte. It also indicates that it possesses a persistently unstable Zn anode/electrolyte interface. After introducing PMN_{-5} additive, the Zn-Zn cell exhibits stable impedance with the laying aside time increases. It can attribute to the dynamic layer formed by the adsorption of PMN_{-5} copolymer macromolecules on Zn anode surface, which blocks water molecules and thereby reduces side-reactions, leading to a stable Zn anode/electrolyte interface.

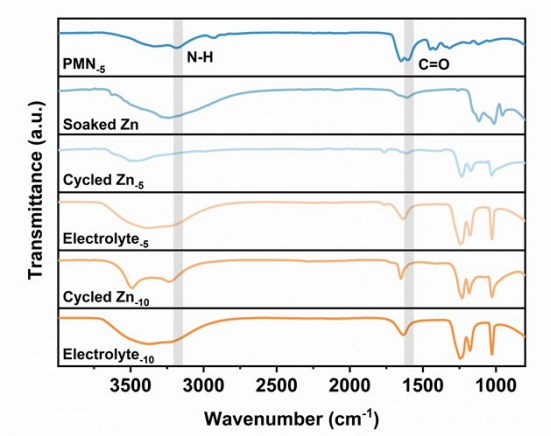

Fig. S14. FTIR spectra of Zn anode and electrolyte after 50 cycles at 5 mA cm^{-2} and 10 mA cm^{-2} current densities using Zn-Zn symmetric cells with PMN_{-5}-containing electrolyte.

Both cycled Zn anode and electrolyte are exhibiting similar characteristic peaks with those of the original PMN_{-5} copolymer and soaked Zn. This indicates that the characteristic groups structure of PMN_{-5} remains intact even under high current densities. Besides, in the FTIR spectra of Zn anode cycled at 5 mA cm^{-2} and 10 mA cm^{-2}, the characteristic peaks of N-H and C=O exhibit a blue shift compared to the original PMN_{-5} copolymer. At 5 mA cm^{-2} current density, the N-H peak shifted from 3185.22 cm^{-1} to 3236.07 cm^{-1} and C=O peak shifted from 1603.21 cm^{-1} to 1650.54 cm^{-1}. At 10 mA cm^{-2}, the peaks of N-H and C=O shifted from 3185.22 cm^{-1} to 3450.27 cm^{-1} and from 1603.21 cm^{-1} to 1613.68 cm^{-1}, respectively. This can be attributed to the chemical adsorption of PMN_{-5} macromolecules on the surface of Zn anode.

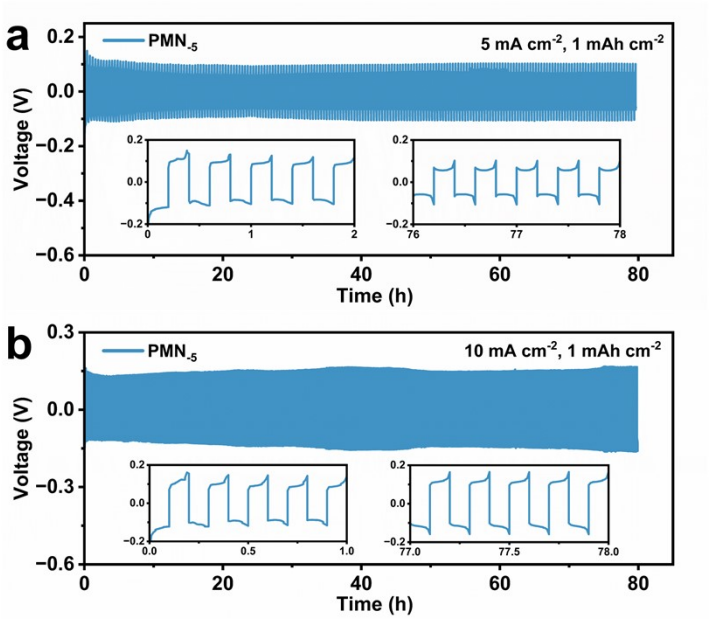

Fig. S15. Cycling performance of Zn-Zn symmetric cells with PMN_{-5}-containing electrolyte at (a) 5 mA cm^{-2} and (b) 10 mA cm^{-2} current densities, respectively.

The Zn-Zn symmetric cells using the same PMN_{-5}-containing electrolyte with FTIR tests also possess good cycling stability under high current densities of 5 mA cm^{-2} and 10 mA cm^{-2}.

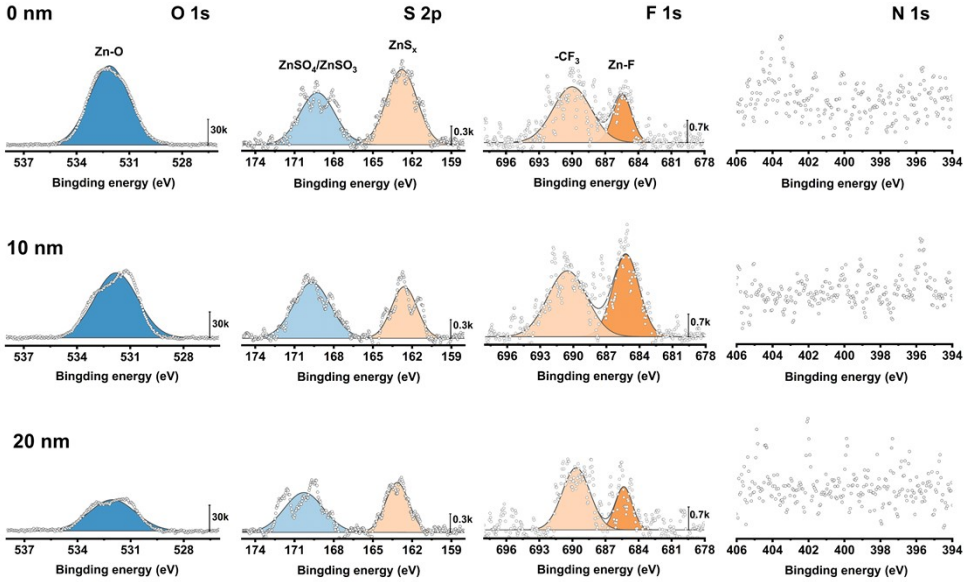

Fig. S16. XPS depth profile for O 1s, S 2p, F 1s, and N 1s of Zn-metal anode surface after 50 cycles in pristine electrolyte at a current density of 5 mA cm^{-2} with a capacity of 1mAh cm^{-2}.

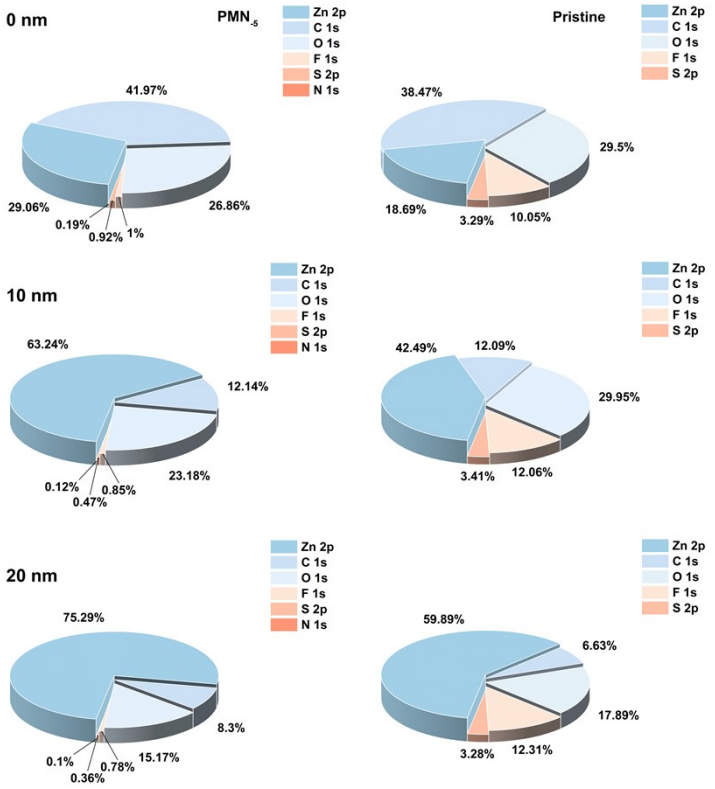

Fig. S17. Evolution of the SEI compositions on surface of the Zn-metal anodes circulating in PMN_{-5}-containing and pristine electrolyte as the etching depth increases.

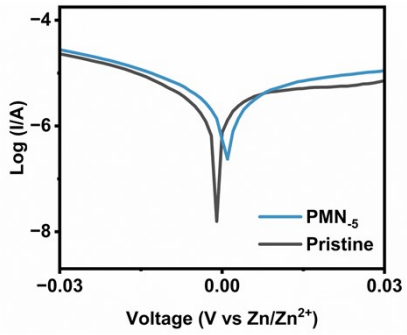

Fig. S18. Tafel plots of Zn-metal anodes tested in pristine and PMN_{-5}-containing electrolyte.

Compared with pristine electrolyte, the corrosion current density decreased from -5.4686 mA cm^{-2} to -5.5765 mA cm^{-2} and the corrosion potential increased from -0.0010 V to 0.0010 V after the addition of PMN_{-5}, which indicates that the corrosion reaction on Zn anode is inhibited and the PMN_{-5} additive has corrosion resistance.

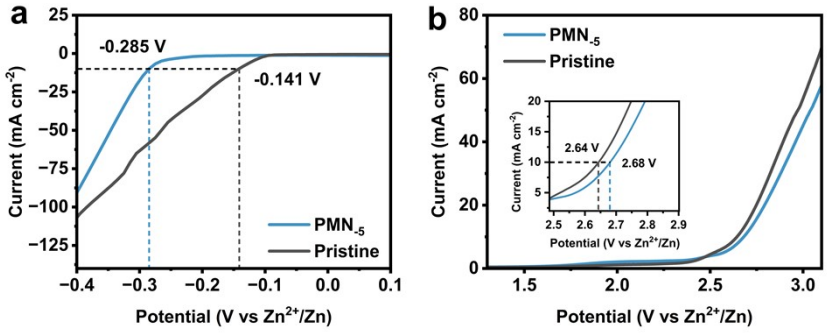

Fig. S19. (a) Hydrogen evolution reaction (HER) and (b) oxygen evolution reaction (OER) curves of different electrolytes determined using LSV at a scan rate of 1 mV s^{-1}.

It can be seen from the figure that PMN_{-5} can reduce the initial potential of HER (from −0.141 V to −0.285 V) and increase the initial potential of OER (from 2.64 V to 2.68 V), indicating that it can inhibit the occurrence of HER and OER.

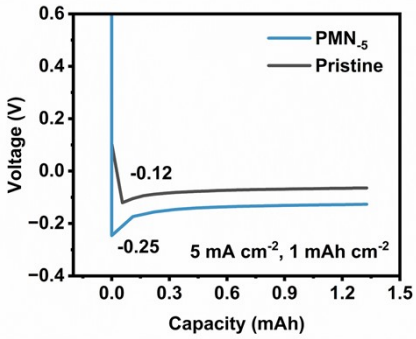

Fig. S20. Initial nucleation overpotentials of Zn plating on Cu electrodes in Zn-Cu asymmetric cells at 5 mA cm^{-2} with different electrolytes.

Compared with the pristine electrolyte, the initial nucleation overpotential increased by 0.13 V after adding PMN_{-5}, which means that more fine zinc-ion nuclei are formed in the electrolyte containing PMN_{-5} and additive enables the deposition more uniform.

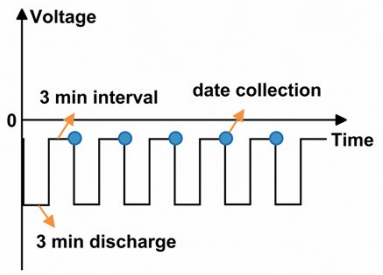

Fig. S21. Measurement setup of the in-situ electrochemical impedance spectroscopy during continuous Zn^{2+} deposition in Zn-Zn symmetrical cells. Each discharge process is separated by a 3 minutes interval, with a total measurement time of 120 min (20 cycles).

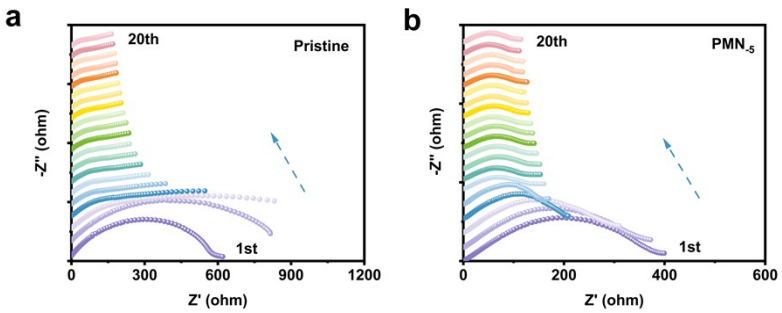

Fig. S22. In-situ EIS of Zn-Zn symmetric cells using (a) pristine and (b) PMN_{-5}-containing electrolyte during electro-plating of Zn^{2+}. Each process last 3 min for charging and 3 min for discharging. The total measurement time is 120 min (20 cycles).

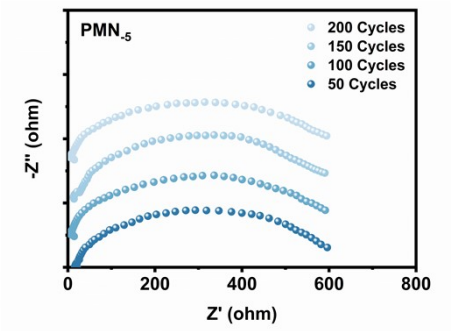

Fig. S23. The impedance plots of Zn-Zn cell after different cycles.

After a series of cycles, the impedance of cell showed no significant changes and maintained a stable state, which is consistent with the results of dynamic in-situ EIS tests. This indicates that after prolonged cycling, the Zn anode/electrolyte interface remains in a stable state, and thus its impedance also remains stable.

Table S1 Molecular weight of copolymers at different molar ratios.

Copolymer	AM:AN (mol: mol)	M_n (g/mol)
PMN_{-4}	96:4	16812
PMN_{-5}	95:5	18668
PMN_{-6}	94:6	17017

Table S2 Energy dispersive spectroscopy (EDS) compositions of Zn-metal anode soaked in PMN_{-5}-containing electrolyte.

Element	Wt.%	Atomic%
N	0.01	0.05
O	10.50	32.06
F	0.07	0.18
S	1.16	1.77
Zn	88.26	65.94
Total	100.00	100.00

Table S3 Comparison cycling performance of Zn-Zn symmetric cells with different additives.

Electrolyte additive	Current density (mA cm^{-2}, mAh cm^{-2})	Cycle life (h)	Ref.
Amino acid D-Phenylalanine (DPA)	5, 1	1200	3
1 M urea + 0.3 M LiOAc	5, 5	435	4
Disodium succinate (SADS)	5, 5	530	5
Protonated triglycine (ggg)	5, 5	400	6
Maltose (Malt)	5, 5	1080	7
Sulfolane (SL)	5, 5	800	8
1,4-dioxane (DX)	5, 5	1000	9
Quaternized lignin (QL80)	5, 5	200	10
Tween-20 (TW20)	5, 5	500	11
PMN_{-5}	5, 1	1840	This work
	10, 1	670	
	20, 1	300	

References

1 F. Wan, L. Zhang, X. Dai, X. Wang, Z. Niu and J. Chen, *Nat Commun*, 2018, **9**, 1656.

2 X. Rui, Y. Tang, O. I. Malyi, A. Gusak, Y. Zhang, Z. Niu, H. T. Tan, C. Persson, X. Chen, Z. Chen and Q. Yan, *Nano Energy*, 2016, **22**, 583-593.

3 A. Naveed, T. Li, A. Ali, F. Ahmad, W. A. Qureshi, M. Su, X. Li, Y. Zhou, J. C. Wu and Y. Liu, *Small*, 2024, **20**, 2401589.

4 X. Feng, P. Li, J. Yin, Z. Gan, Y. Gao, M. Li, Y. Cheng, X. Xu, Y. Su and S. Ding, *ACS Energy Letters*, 2023, **8**, 1192-1200.

5 Y. Ding, L. Yin, T. Du, Y. Wang, Z. He, J. A. Yuwono, G. Li, J. Liu, S. Zhang, T. Yang and Z. Guo, *Advanced Functional Materials*, 2024, **34**, 2314388.

6 J. Zhang, Y. Liu, Y. Wang, Z. Zhu and Z. Yang, *Advanced Functional Materials*, 2024, **34**, 2401889.

7 Y. Liu, B. Xie, Q. Hu, R. Zhao, Q. Zheng, X. Huang, S. Deng, Y. Huo, J. Zhao, B. Xu and D. Lin, *Energy Storage Materials*, 2024, **66**, 103202.

8 T. Wei, X. Zhang, Y. Ren, Y. Wang, Z. Li, H. Zhang and L. Hu, *Chemical Engineering Journal*, 2023, **457**, 141272.

9 T. Wei, Y. Ren, Y. Wang, L. Mo, Z. Li, H. Zhang, L. Hu and G. Cao, *ACS Nano*, 2023, **17**, 3765-3775.

10 J. Xu, M. Wang, M. Asraful Alam, T. K. A. Hoang, Y. Zhang, H. Li, Y. Lv, A. Zhao and W. Xiong, *Fuel*, 2023, **333**, 126450.

11 Q. Deng, S. You, W. Min, Y. Xu, W. Lin, J. Lu and C. Yang, *Advanced Materials*, 2024, **36**, 2312924.